Antenna Control System Using Step Tracking Algorithm with H_∞ Controller

Chang-Ho Cho, Sang-Hyo Lee, Tae-Yong Kwon, and Cheol Lee

Abstract: The outdoor antenna servo system is subject to has significant torque disturbances from wind pressures and gusts on the antenna structures, as well as bearing and aerodynamic frictions. This control system should provide a sharp directivity in spite of the environmental disturbances and internal uncertainties. Therefore, the implementation of a real-time controller is necessary for the precise generation of the reference signal and robust tracking performance. In this paper, the discrete-time controller for the quick tracking of a target communication satellite is designed by applying the sampled-data H_∞ control theory along with the reference signal generated by an improved conventional step-tracking algorithm. The sampled-data H_∞ controller demonstrates superior robustness for the longer sampling period when compared with a simple PID controller.

Keywords: H_∞ control, sampled-data system, step tracking, satellite antenna.

1. INTRODUCTION

The satellite broadcast receiving system shown in Fig. 1, consists of a satellite parabola antenna, an LNB (Low-Noise Block-Down) converter, and a set-top box tuner that sends signals to a TV set.

In order to receive signals efficiently from the Koreasat (Mugunghwa) satellite, particularly, on a mobile satellite communication system, a satellite antenna should track a target satellite accurately by means of a tracking controller [1]. One of the conventional tracking controllers is a step-tracking controller that works on the principle by periodically "jogging" of the antenna up/down and clockwise/counter-clockwise for re-positioning to the point of maximum signal reception .

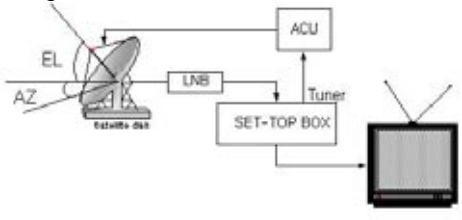

Fig. 1. Configuration of DBS system.

Manuscript received December 5, 2001; accepted December. 5, 2002. The present research has been conducted by the Research Grant of Kwangwoon University in 2000.

Chang-Ho Cho and Sang-Hyo Lee are with the Information & Control Engineering Department, Kwangwoon University, Korea. (e-mail: cch486@yahoo.co.kr, sh41lee@daisy.gwu. ac.kr).

Tae-Yong Kwon is with the National Star, Co., Korea. (e-mail: nationalkwon@hanmail.net).

Cheol Lee is with the Finix System, Co, Korea. (e-mail: cdobub@empal.com).

In this paper, in order to develop and experiment with an antenna tracking control system, Korea Telecom's Koreasat-3 (Mugunghwa-3), which is easily observable in the entire Korean Peninsula, has been used as the target satellite. Koreasat-3 is configured to provide both fixed and direct broadcast services, doubling the capacity of both Koreasat-1 and Koreasat-2. Specifically, Koreasat-3 has 24 Ku bands (Fixed Satellite Service), 6 Ku bands (Direct Broadcast Service), and 3 Ka bands transponders. It also features a steerable antenna that provides regional coverage capability. Its 3° beam directivity can cover the majority of India, and the most densely populated portions of China, or Japan. The satellite is positioned at 116° east [2].

Generally, parabola antennas or offset-parabola antennas are used to receive satellite broadcasts, but recently, easily installable flat-lightweight antennas have been developed and adopted. Since receiving antennas for Koreasat-3 should have a circular polarization patch feature and should be installed on a mount, a small lightweight and easily installable antenna is preferred. High gain, sharp directivity, and high efficiency are important criteria for the antennas [3].

In this paper, the receiving regions are restricted to the Korean Peninsula and variations of the antenna azimuth angle are considered only when on a movable vehicle. Under these conditions, the purpose of the research is (i) to develop a system where azimuth and elevation angles of the antenna mount are controlled only by a step tracking algorithm without any costly sensor; (ii) to design a robust digital positioning controller to receive direct broadcasts more economically and efficiently; (iii) to observe how the

step size variations influence the stability and tracking performance of the antenna mount.

2. ANTENNA TRACKING ALGORITHMS

The basic tracking method used in this research is the so-called step-tracking algorithm proposed in [4]. The step tracking operation begins when the antenna is commanded to make an initial one-step turn in any direction, after which the level of the receiving signal is compared with the previous level before the turn. If the signal level has increased, the antenna continues another one-step turn in the same direction. If the signal level has decreased, the turn of the antenna is reversed. By these step-by-step turns, the receiver antenna can track the point of maximum signal level. Since this method uses only the feedback information of the electric field intensity, it has advantages of an economic hardware configuration and a relatively simple control software.

In practice, the step-tracking operation should be performed uniformly toward the possible space where the target satellite may exist after adequately determining the order of the traversal and longitudinal turnings. That is, the step tracking method requires a fundamental algorithm that can decide the direction of the movement to provide increased signal level by comparing the previously memorized input signal level with the most recently received signal level after turning step angles. Effort should be made to obtain an optimal step algorithm on which the tracking performance of the antenna depends. Also, the step tracking system assumes that the antenna is located in a position where it is possible to receive the beacon signal from the target satellite. Therefore, the information of both the previously known position and the present position of the target satellite obtained by sophisti-cated sensors like the GPS or the flux gate is usually required for the antenna tracking system [5].

To meet these requirements, this study will show that a satellite receiving system can be configured using step-tracking algorithm with an attached pre-scan

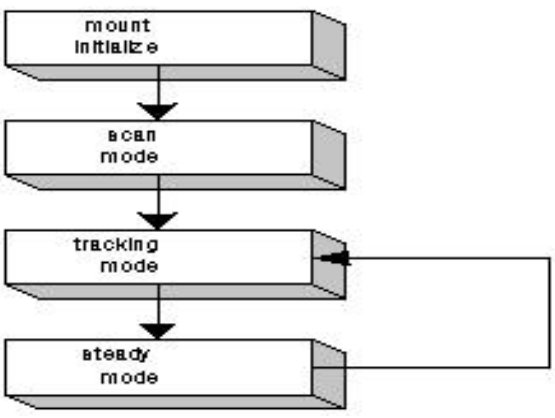

Fig. 2. Block diagram of tracking system.

movement. This economic and efficient receiving system can operate without any expensive sensors.

The step-tracking procedure may be divided into several stages, the operation for each stage defined as shown in Fig. 2.

The initial mode of the defined operation is the preparatory stage of a scan mode where the elevation angle of the mount turns 42° with respect to the horizontal plane and the azimuth angle turns to the initial position 0° of the mount.

At the scan mode, the antenna captures the beacon signal of the satellite and executes the operation to find the region where the full step tracking is possible. The region of scan is defined as the elevation angle of 42°-51°, and the azimuth angle of the range from −177.5° to + 177.5°. That is, the antenna moves the elevation angle 3°, which is determined by considering the angle of half power gain and the scan velocity, after the azimuth angle moves from −177.5° to + 177.5° clockwise, and then the azimuth angle moves again counterclockwise. This procedure is repeated until it finds the position where the step-tracking is possible as shown in Fig. 3.

During the scan mode, the reference trajectory, as shown in Fig. 3, is generated and used for the tracking control of the antenna mount. The scan mode ends after memorizing the point with the peak AGC (Auto Gain Control) gain. This point is used as a new reference input for another tracking mode.

The need for the scan mode before the step-tracking mode is due to the sharp directionality of the satellite antenna. Since the antenna gain variation is sensitive within the narrower range, the tracking mode cannot be executed in advance. The results of the repeated experiments have shown that the range of the AGC output voltage lies between 0.5 [V] and 3.2 [V], and the range of the tracking mode spans narrowly under 10° in case of the azimuth angle.

At the tracking mode, the antenna is controlled to track one-step toward the satellite to obtain the higher receiving level. If the antenna arrives at the level where the broadcast can be fully received, the stop drive mode is executed.

The stop drive mode is executed to avoid mechanical damage as the desired receiving level is obtained. During the antenna stop operation, the processor continually receives the levels of the signal received. When the level of the measured signal decreases under the reference value due to the disturbances or un-

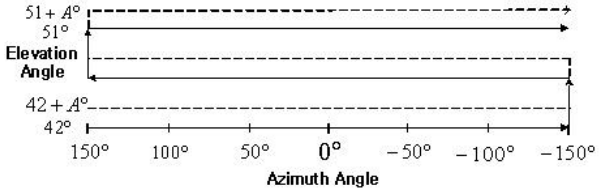

Fig. 3. Scan mode trajectory.

expected movements of the antenna, the scan mode begins again. The level of the signal is measured by utilizing the AGC output voltage of the tuner. The step- tracking algorithm applied to the tracking mode is implemented according to the sequences of right, up, left, and down.

3. IDENTIFICATION OF TRANSFER FUNCTIONS OF THE MOUNT SYSTEM

In this paper, the mount of the antenna position system consists of two geared DC motors connected to the axes for the elevation angle, θ_1, and the azimuth angle, θ_2, respectively. Other than the gear ratios of 3600:1 for the elevation and 1800:1 for the azimuth, the two DC motors have the same specifications.

The transfer functions of the mount system should have been obtained from the overall model consisting of the antenna mount, and the servo driver with power amplifiers. The mathematical model contains some errors originating from the uncertainties in measured parameters, unmeasured parameters such as mechanical frictions, and any missing information of some component parts. The system identification toolbox of CEMTOOL has been used to solve these problems. The procedure used to model a dynamical system from the observed input-output data involves three basic ingredients: the input-output data, a set of candidate models with model structures, and a criterion to select a particular model in the set of identified models [6]. Specifically, the CEMTOOL and DSP/IO board performs data acquisition and model estimation. The estimation model structure is selected as an ARX (autoregressive model with exogenous input) model [7] shown in(1).

$$A(q)y(t) = B(q)u(t-uk) + e(t). \tag{1}$$

The parameters of the ARX model structure are estimated using the least square method. The periodic triangular waves are applied to the physical system as a test signal, after which the angular displacements of the azimuth and elevation components of the mount are measured as the outputs. With 3000 data points of input and output, the ARX algorithm of the CEMTOOL has obtained the transfer function.

The geared motors, JEIL BSM-0615-DV24, are used in the experiment and the overall transfer functions from the motor input voltage $\boldsymbol{E(s)}$ to the mount angles $\theta_1(s)$, $\theta_2(s)$ are obtained using (2) and (3).
Elevation:

$$\frac{\theta_1(s)}{E(s)} = \frac{-0.1s^2 + 11.7s + 2950}{s^3 + 70s^2 + 11483s - 49}. \tag{2}$$

Azimuth:

$$\frac{\theta_2(s)}{E(s)} = \frac{-01.2s^2 - 59.6s + 4898}{s^3 + 60s^2 + 11483s - 49}. \tag{3}$$

The transfer functions obtained are approximated as 3rd-order systems, and their Bode diagrams are shown in Fig. 4. As expected, the two transfer functions show nearly equal frequency responses since the difference of the mechanical load components of the antenna mount system should make few contributions to each transfer function because of the high gear ratios of the azimuth and elevation components of the mount.

4. DESIGN OF PID CONTROLLER AND SAMPLED-DATA H_∞ CONTROLLER

4.1. Design of PID controller

In this paper, PID controllers popularly used in industrial fields are designed as reference controllers to compare with H_∞-robust controllers, which are designed to have similar characteristics in performance and robustness. PID controllers to be designed have the structure of a typical feedback control system shown in Fig. 5. The parameters, $\boldsymbol{K_P}$, $\boldsymbol{K_I}$, $\boldsymbol{K_D}$, of the three-term controllers are designed adhering to the following performance specifications.

For the 6 degree reference displacement input :
Settling time: less than 2 seconds,
Overshoot: less than 5%,
Steady state error: less than 1%.

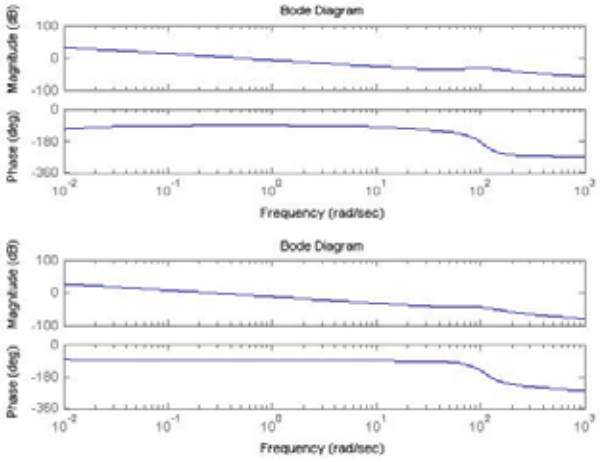

Fig. 4. Frequency response of the AZ and EL model.

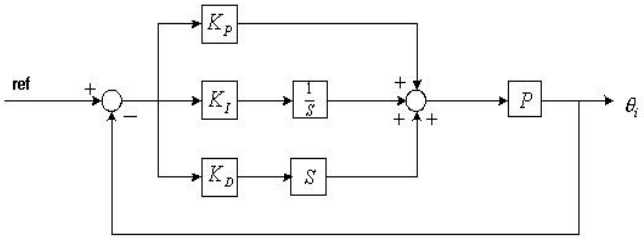

Fig. 5. Design structure for a PID controller.

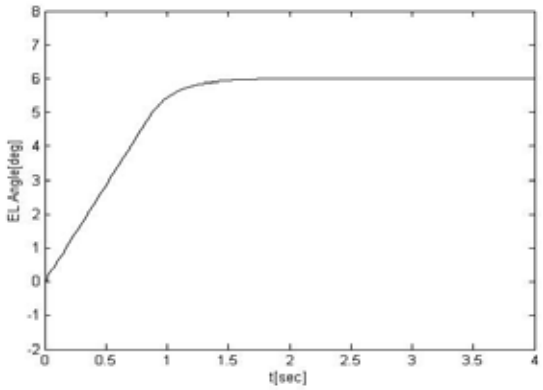

Fig. 6. Step response of PID control system: EL angle, □[rad] for time[sec].

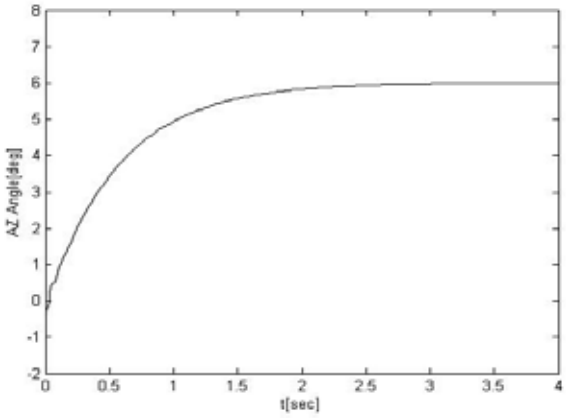

Fig. 7. Step response of PID control system: AZ angle, □[rad] for time[sec].

Gains (K_P, K_I, and K_D) are determined by the iteration method observing control performances for each gain candidate using the for-loop algorithm, and the results are obtained using (4) and (5).
Elevation:

$$K_P = 20, \quad K_I = 0.0004, \quad K_D = 0.001 \tag{4}$$

Azimuth:

$$K_P = 4, \quad K_I = 0.00015, \quad K_D = 0.001 \tag{5}$$

Figs. 6 and 7 show the simulation results for the two PID controllers, both of which show step responses satisfying the design specifications.

4.2. Design of the discrete-time H_∞-robust controllers

An H_∞-robust controller is designed for the plant of the satellite receiving antenna system. The controller is designed by representing the mathematical model of the plant, and then discretizing the model by the 7-stage H_∞-discretization using the lifting technique proposed by Chen and Francis [8, 9, 10].

In this paper, to design the discrete-time controller for the satellite antenna system to allow for robust tracking of the reference signal, the optimal sampled-data (SD) control theory is used [8]. The optimal sampled-data control theory is practically used to solve various problems that arise when a continuous-time H_∞ controller is transformed to a discrete-time controller. This theory also referred to as "a direct design method by lifting" helps to design a discrete-time H_∞ controller based on the continuous-time H_∞- robust control theory and has the prime advantage of little performance deterioration for the longer sampling period. The procedure for Chen and Francis' design method is as follows: to begin, an equivalent finite-dimensional I/O discrete-time system is obtained from a sampled-data control system through using computational steps, which is again transformed into a fictitious continuous-time system with the preserved H_∞-norm by bilinear transformation. Then, the continuous-time H_∞-optimal controller is designed using the established H_∞ control method.

Finally, the discrete-time H_∞-optimal controller is obtained from the continuous-time H_∞-optimal controller by the bilinear transformation.

In this paper, in order to implement the controller mentioned above, the design procedures include the MATLAB codings of the computational steps in [8].

The H_∞-optimal control problem is formulated for the structure of the generalized plant including the weight functions, W_{g1}, W_{g2}, and W_{g1}.

To design the H_∞-controllers, an integrator was inserted to enhance time-response characteristics and steady-state error reduction and to enable the CEMTOOL simulation experiments. The weight function of the integrator output W_{g1} is used to determine the transient and steady-state perform ances of the controller. The weight function of the disturbance input W_{g2} is adjusted to increase robustness for the uncertainties of the system parameters. W_{g3} is set to limit the control signal from the physically implemented controller. The design specifications for the H_∞-controllers are the same as those of PID controllers, and weight functions are restricted to real constants and determined by the iteration method to obtain H_∞-controllers equivalent to the PID performance specifications. The weight functions are obtained using (6) and (7).
Elevation:

$$W_{g1} = 24, \quad W_{g2} = 0.09, \quad W_{g3} = 5 \tag{6}$$

Azimuth:

$$W_{g1} = 30.11009, \quad W_{g2} = 0.00447, \quad W_{g3} = 38.09 \tag{7}$$

When 10 [ms] sampling time is used, the H_∞-optimal sampled-data controllers designed by Chen and Francis' procedure for the structure in Fig. 8 are found as:
Elevation:

$$K_{\theta_1} = \frac{0.2466z^2 + 3.451z^{-6} - 0.2466}{z^2 - 1.885z + 0.8851} \tag{8}$$

Azimuth:

$$K_{\theta_1} = \frac{0.7309z^2 - 1.893z^{-6} - 0.7309}{z^2 - 0.9467z - 0.05325} \quad (9)$$

Figs. 9 and 10 represent step responses of the H_∞ control system by simulation. These results show good tracking performance.

5. PHYSICAL EXPERIMENT OF ANTENNA SYSTEM

The satellite antenna tracking system is physically implemented as shown in Fig. 11. The tuner selects a channel of the desired frequency from the received antenna signals with the AGC output proportional to the received signal level. The AGC output voltage usually lies between 2.65 [V] and 3.22 [V], which is amplified and filtered by a low-pass filter into the range between 0 [V] and 5 [V]. Any amplified voltage within this range is applied to the A/D converter as a reference voltage.

The A/D converter with 12 bit resolution is used to detect the amplified AGC signal and the motor position signals. The input voltage of the DC driving motors is set to 24 [V], where the angular velocity of the elevation drive is set to 6[°/s] and the angular velocity of the azimuth drive is set to 11[°/s].

The real-time controllers are implemented using the CEMTOOL software and the DSP/IO board (RG-DSPIO) supplied by REALGAIN Co. Block algorithms are transformed into C codes by AUTOTOOL DSPIO) supplied by REALGAIN Co. Block algorithms are transformed into C codes by AUTOTOOL in CEMTOOL and downloaded to the DSP board in order to execute the experiments. The specifications of the DSP/IO board are shown in Table 1.

The parabola antenna and mount system shown in photos 1 and 2 have specifications as shown in Tables 2 and 3, respectively.

Figs. 12 and 13 show the antenna pointing trajectories according to the variations of the elevation and azimuth angles of the antenna mount after scanning the tracking range once.

In cases where PID controllers are used, greater vibration in the mount are observed. The sampled-data H_∞-robust controllers show better tracking performances than the PID controllers. In the case of the PID

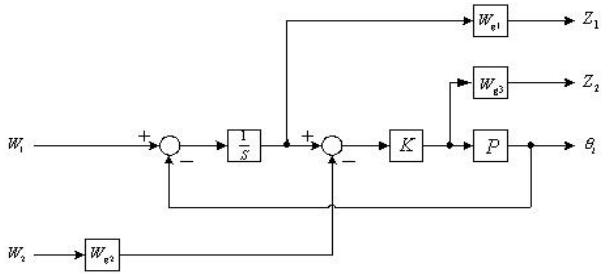

Fig. 8. Design structure for H_∞ controller.

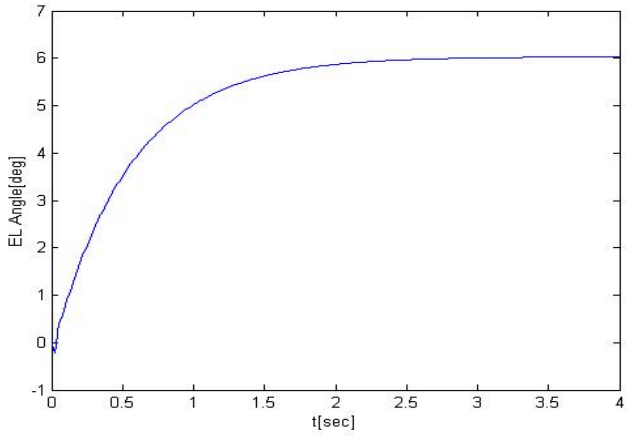

Fig. 9. Step response of H_∞ control system: EL angle, □[rad] for time[sec].

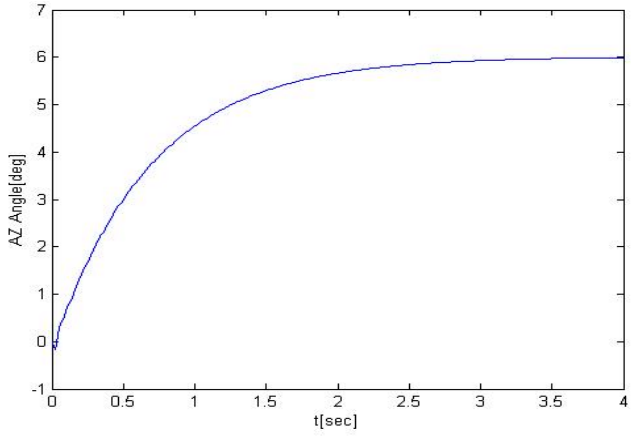

Fig. 10. Step response of H_∞ control system: AZ angle, □[rad] for time[sec].

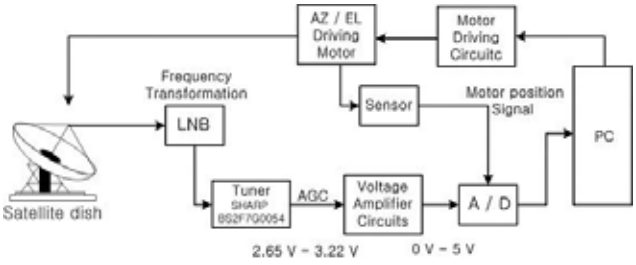

Fig. 11. Block diagram of experiments configuration.

Table 1. Specifications of DSP/IO(RG-DSPIO).

Item	RG-DSPIO01	Values
Processor	Main Processor	TMS320C32
	Operating Frequency	60 MHz
	Internal Cache	256 bytes
	Number of Timer	2
Memory	ROM	128 Kbytes
	Normal SRAM	128 or 512 Kbytes
	fast RAM	256 Kbytes
Interface		256 Kbytes

Photo 1. Experimental setup of the mount and antenna.

Photo 2. Experimental setup of the real-time control system.

Table 2. Specifications of antenna.

Specifications	Values
Diameter	60 [cm]
Aperture efficiency	74 [%]
Antenna half-power angle	2.95 [°]
Maximum receiving gain	36.13 [dBi]

Table 3. Specifications of mount.

Specifications	Values
Dc servo motor	JEIL BSM-0615-DV24 rated voltage: 24 [V] gear ratio: 3600: 1, elevation 1800: 1, azimuth
Drive velocity	elevation: 5 [°/ s] azimuth: 10 [°/ s]
Range of Rotation	elevation: 0° ~ 60° azimuth: 0° ~ 355°
Payload	30 [kg] maximum
Dimensions	L×H×W = 270[mm]×245[mm] ×240[mm]
Potentiometer	resolution: 0.025[%], 10[turn], 5[k□] taper linearity: ±0.2[%]

control, the vibration phenomena are related to the sampling period and the derivative term controller. While during a shorter sampling period the vibrations associated with the use of the PID control decrease, the sampled-data H_∞-robust controller is less sensitive. In Figs. 14 and 15, elevation angle versus time during the scan mode are shown. Amplitudes of vibrations in cases where PID controllers are used two times greater than the sampled-data H_∞-robust controllers.

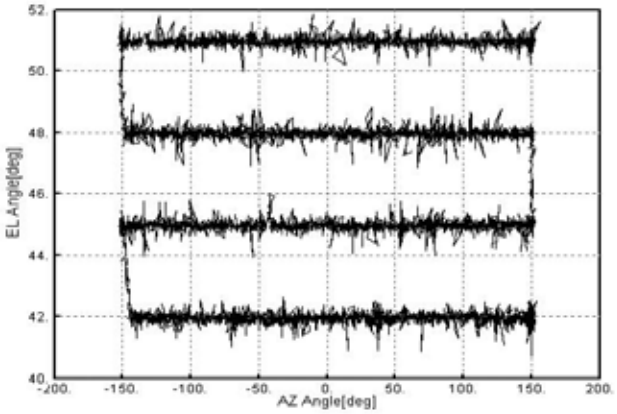

Fig. 12. EL vs. AZ angle with PID controller.

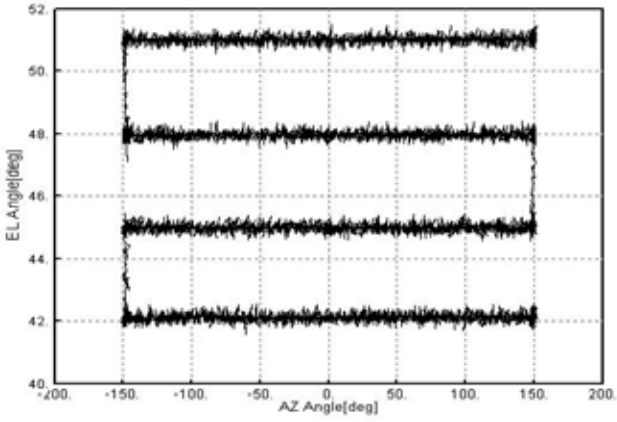

Fig. 13. EL vs. AZ angle with H_∞ controller.

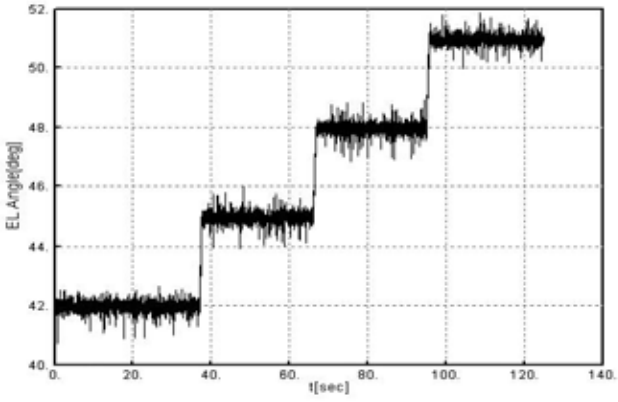

Fig. 14. EL angle vs. time with PID controller.

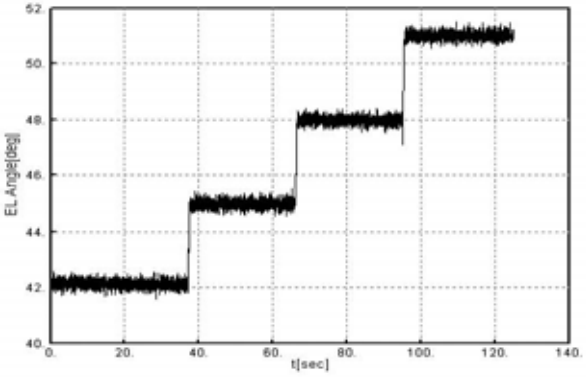

Fig. 15. EL angle vs. time with H_∞ controller.

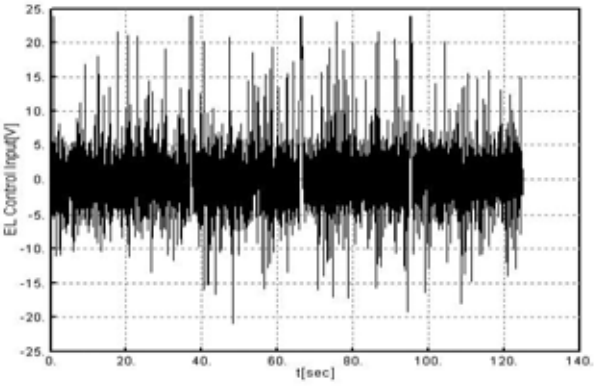

Fig. 16. EL Control input vs. time with PID controller.

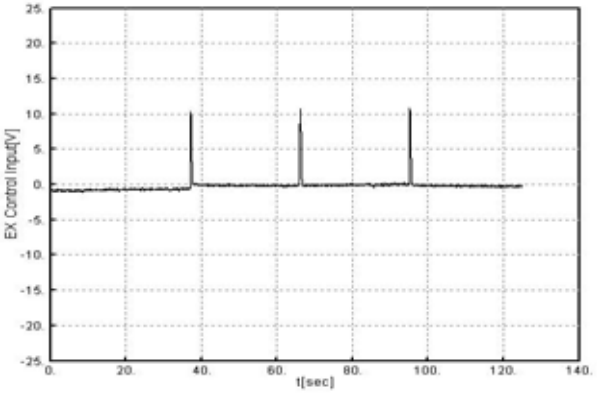

Fig. 17. EL control input vs. time with H_∞ controller.

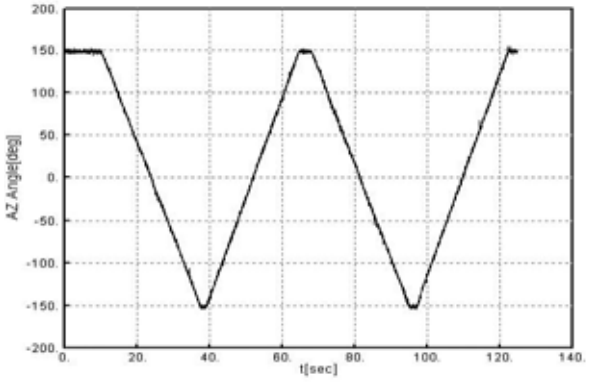

Fig. 18. AZ angle vs. time with PID controller.

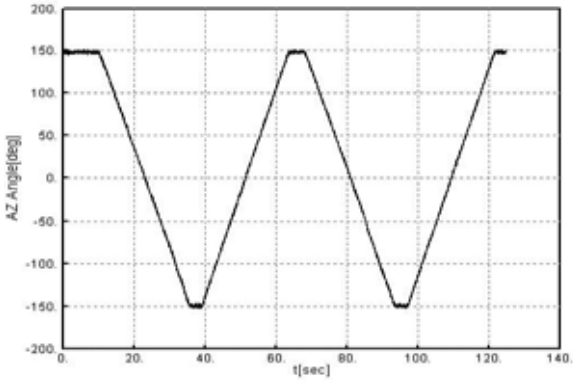

Fig. 19. AZ angle vs. time with H_∞ controller.

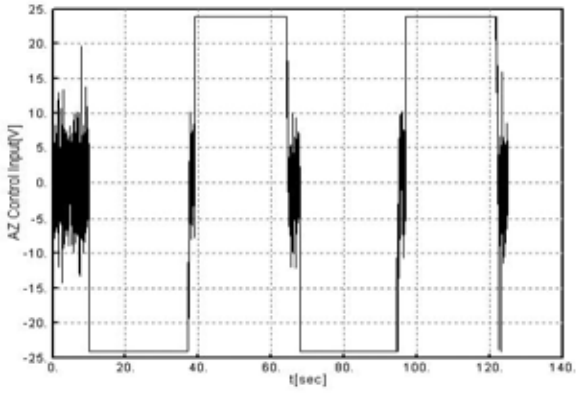

Fig. 20. AZ control input vs. time with PID controller.

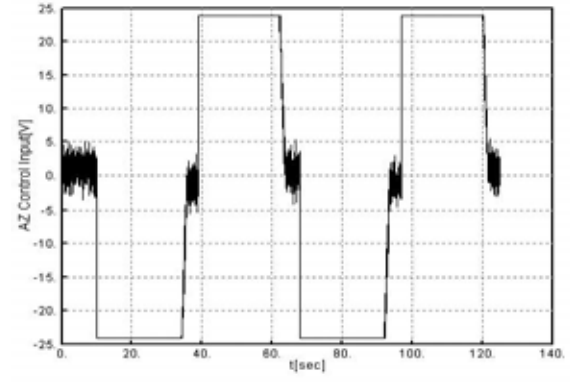

Fig. 21. AZ control input vs. time with H_∞ controller.

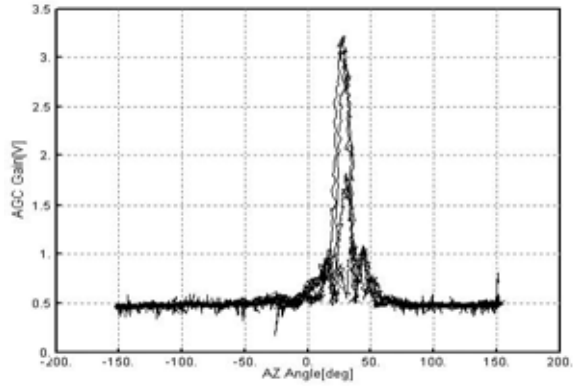

Fig. 22. AZ angle vs. AGC gain with PID controller.

In Figs. 16 and 17 the outputs of the controllers are compared for the scan mode executions as shown in Figs. 14 and 15. In the transient periods, control outputs from the PID controllers are verified to be four times greater than those from the sampled-data H_∞-robust controllers. In Fig. 16, it is observed that the control signal of the PID controller is the main cause of the greater vibrations of the antenna mount as shown in Fig. 14.

Figs. 18 and 19 show the azimuth angle versus time during the scan mode, and Figs. 20 and 21 show controller outputs from the controllers during the scan mode execution shown in Figs. 18 and 19. Where PID controllers are used, variation levels of the azimuth angles are less than those of the elevation angles, but the controller outputs from PID controllers are two times as great.

In Figs. 22 and 23, variations of the AGC voltage according to variations of the azimuth angles are shown. During executions of the scan mode, the maximum AGC gain was about 3.2 [V].

Although this value depends on location and weather conditions, the results of the physical experiments show that, with the AGC gain of 3 [V], satellite broadcasts can be satisfactorily received. During the scan mode executions, it was able to raise the AGC gain to 3.5 [V] maximum.

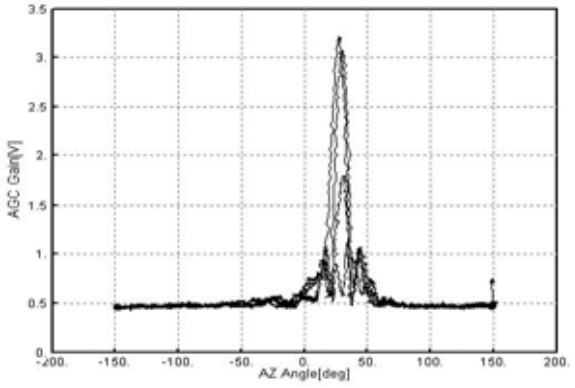

Fig. 23. AZ angle vs. AGC gain with H_∞ controller.

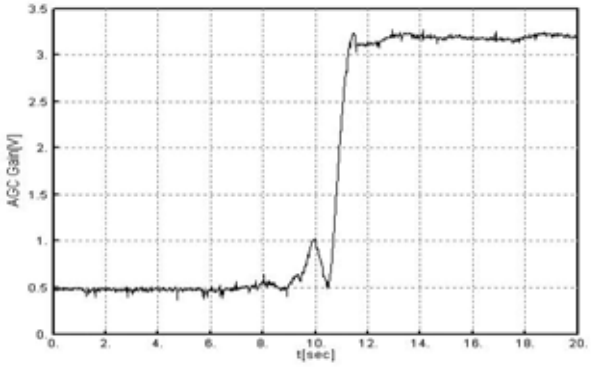

Fig. 24. Time vs. AGC gain with PID controller at tracking mode.

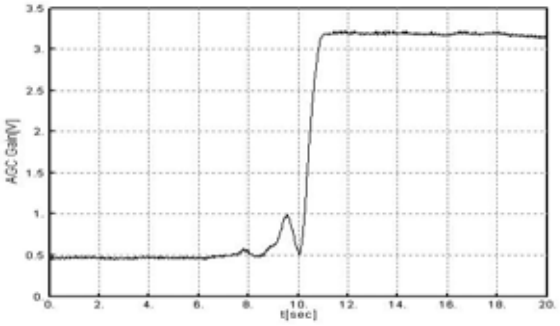

Fig. 25. Time vs. AGC gain with H_∞ controller a tracking mode.

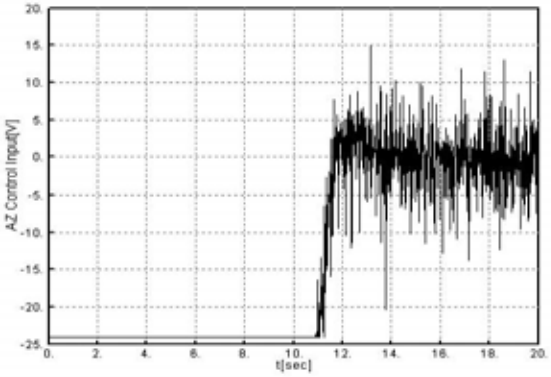

Fig. 26. AZ control input vs. time with PID controller at tracking mode.

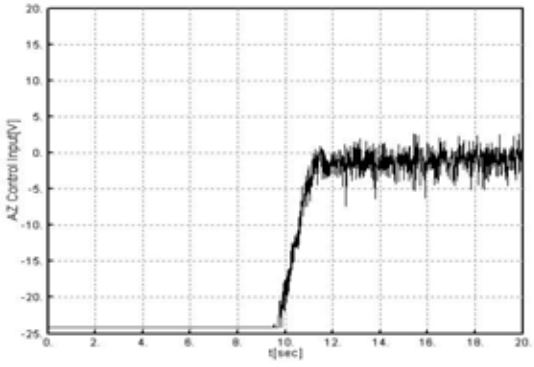

Fig. 27. AZ control input vs. time with H_∞ controller at tracking mode.

In Figs. 24 and 25, variations of the AGC voltage versus time during the tracking mode executions are shown. In the neighborhood of the point of 10 [s], the time to reach the target is observed 0.7 [s] faster in case of H_∞-robust controllers and the AGC gain curve is flatter than in case of PID controllers.

Figs. 26 and 27 show the controller outputs for the azimuth components, during the tracking mode executions. These controller outputs for the elevation and azimuth components correspond to the tracking mode executions as shown in Figs. 24 and 25.

In Figs. 28 and 29, the azimuth and elevation angles, as well as the AGC receiving gain after both the scan and the tracking mode executions are shown in

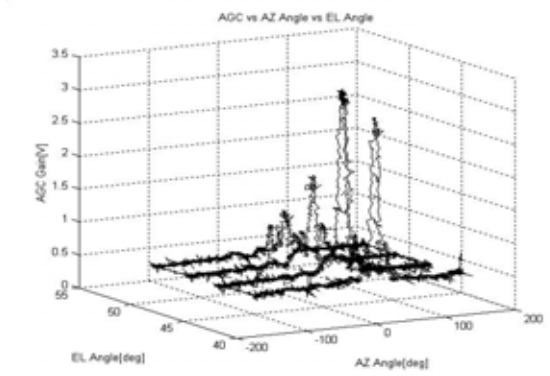

Fig. 28. AGC gain for EL and AZ angle with PID controller.

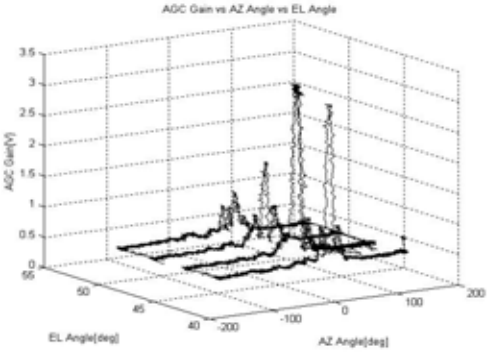

Fig. 29. AGC gain for EL and AZ angle with H_∞ controller

3D plots.

To summarize the results of the physical experiments, the PID controller was found to have more vibrations than the sampled-data H_∞-robust controller. The deterioration of the overall tracking performance was consequently observed, although the vibrations decrease for the shorter sampling periods. The cause of these vibrations is related to the sampling period of 10 [ms] and the derivative term of the PID controller. In case of the PID controller, fewer vibrations in the azimuth component were observed than were found in the elevation component due to the different sensitivities of the two components. The sensor in the azimuth component has less noise sensitivity for the wider range between $-177.5°$ and $+177.5°$. Conversely, the sensor in the elevation component has the larger noise sensitivity for the relatively narrower range between $0°$ and $60°$.

The sampled-data H_∞-robust controller was observed to be less sensitive both to the variation of the sampling period and the noise from the feedback sensors of the azimuth and elevation components showing the robust tracking performances. This robustness comes from the sampled-data H_∞-robust controller designed by the method proposed by Chen and Francis [8], which has superior robustness for the longer sampling period. Therefore, in this paper, it is proved that the sampled-data H_∞-robust controller is a useful tool for the physical plant with constraints and uncertainties not easily identified in the simulation.

6. CONCLUSIONS

Generally, the antenna tracking system using the step- tracking algorithm requires additional sensors such as a position information sensor and a receiving signal level sensor to obtain the stable and fast tracking performance. Since the system requires a sharp directivity, its tracking controller should be able to track the reference signal in spite of environmental disturbances and internal uncertainties. These requirements of additional sensors and an accurate controller result in increased cost for the system in total.

In this paper, by modifying the step algorithm to meet receiving conditions in the Korean Peninsula, we have attempted to develop an antenna system capable of quickly and accurately tracking the target satellite Koreasat and receiving of the signal transmitted from it without using any additional sensors.

In the physical experiment, using only the AGC voltage to detect the receiving level, the proposed algorithm and controller demonstrated the desired performances. Particularly, it was verified that the discrete-time H_∞-robust controllers show robust performances superior to the PID controllers for the longer sampling period, although the H_∞-robust controllers were designed with simplified real constant weight functions.

Furthermore, in implementing the step algorithm, it was verified that the performance of the antenna tracking system largely depends on step sizes through repeated experiments. Further work is needed to design attitude correction systems using the improved tracking algorithm and minimum number of sensors in order that surface vehicles such as ships may receive satisfactory satellite broadcasts during movement.

REFERENCE

[1] G. J. Hawkins, D. J. Edward, and J. P. McGeehan, "Tracking system for satellite communication," *IEE Proc.,* vol. 135, part F, no. 5, pp. 393-407, 1988.

[2] J. S. Seo, "Direct DBS," Seminar for a Present Condition and View of the Multimedia Communication Service Technology, KICS, pp. 27-38, 1996.

[3] G. Maral and M. Bousquet, *Satellite Communication System 3/e*, John Wiley & Sons Ltd, 1998.

[4] N. N. Tom, "Auto-tracking of communication satellites by the step-track technique," *IEE Conference Proc. on Earth Station Technology*, pp. 121-126, 1970.

[5] J. C. Choi, *A Study of Satellite Tracking System of DBS Receiving Antenna on Shipboard*, Korea Maritime University Ph. D Dissertation, 1998.
[6] L. Ljung, *System Identification Toolbox User's Guide,* The Math Works, Natick, 1998.
[7] L. Ljung, *System Identification: Theory for the User,* Prentice-Hall, Englewood Cliffs, 1987.
[8] T. Chen and B. Francis, *Optimal Sampled-Data Control Systems*, Springer, London, 1995.
[9] T. Chen and B. Francis, "H_∞-Optimal sampled-data control: computation and design," *Automatica*, vol. 32, no. 2, pp. 223-228, 1996.
[10] B. Bamieh and J. B. Pearson, "A general framework for linear periodic systems with application to H_∞ sampled-data control," *IEEE Trans. on Automat. Control*, vol. 37, no. 4, pp. 418-435, 1992.
[11] P. Gahinet, A. Nemirovski, and A. J. Laub, *LMI Control Toolbox User's Guide*, The Math Works, Natick, 1995.
[12] K. Zhou, J. C. Doyle, and K. Glover, *Robust and Optimal Control*, Prentice-Hall New Jersey, 1996.

Chang-Ho Cho received the Master of Engineering degree from the Department of Control and Instrumentation, Kwangwoon University in 2000. Dr. Cho. completed Ph.D. degree in the Department of Information & Contro Engineering Kwangwoon University in 2002. He is currently a senior engineer at National Star Company.

Sang-Hyo Lee received the Ph.D. degree in Engineering from the Department of Electrical Engineering from Yonsei University in 1981. He became an assistant professor in the Department of Electronic Engineering at Kwangwoon Unversity in 1980. He is now a professor in the Department of Control and Instrumentation Engineering, Kwangwoon University.

Tae-Yong Kwon received the M.S. degree in Engineering from the Department of Electronic Engineering, Kwangwoon University in 1987. He completed the Ph.D. course in the Department of Information & Control Engineering, Kwangwoon University. He is the president of National Star, a venture company.

Cheol Lee received the M.S. degree in Engineering from the Department of Electrical Engineering, Kwangwoon University in 1991. He completed his Ph.D. program in the Department of Information and Control Engineering, Kwangwoon University in 2002. He worked as an engineer at Dae Ryung Precision Company in 1990. He is nowthe director of Finix.